

A NEW YOUNG GALACTIC SUPERNOVA REMNANT CONTAINING A COMPACT OBJECT: G15.9+0.2

STEPHEN P. REYNOLDS,¹ KAZIMIERZ J. BORKOWSKI,¹ UNA HWANG,² ILANA HARRUS,² ROBERT PETRE,² AND GLORIA DUBNER³

Received 2006 July 21; accepted 2006 October 10; published 2006 November 6

ABSTRACT

We identify the radio-emitting shell-type supernova remnant G15.9+0.2 as a relatively young remnant containing an X-ray point source that may be its associated neutron star. The integrated spectrum of the remnant shell obtained from our 30 ks exploratory *Chandra* observation shows very strong lines that require elevated element abundances from ejecta, in particular of sulfur. A plane-shock model fit gives a temperature $kT = 0.9$ (0.8, 1.0) keV, an ionization timescale $n_e t = 6$ (4, 9) $\times 10^{10}$ cm⁻³ s, and a sulfur abundance of 2.1 (1.7, 2.7) times solar (90% confidence limits). Two-component models with one solar and one enriched component are also plausible, but they are not well constrained by the data. Various estimates give a remnant age of order 10³ yr, which would make G15.9+0.2 among the dozen or so youngest remnants in the Galaxy. The sparse point-source spectrum is consistent with either a steep $\Gamma \sim 4$ power law or a $kT \sim 0.4$ keV blackbody. The spectrum is absorbed by a H column density $N_H \sim 4 \times 10^{22}$ cm⁻² similar to that required for the remnant shell. The implied 2–9.5 keV source luminosity is about 10³³ ergs s⁻¹ for an assumed distance of 8.5 kpc consistent with the high absorption column. We suggest that the point source is either a rotation-powered pulsar or a compact central object.

Subject headings: ISM: individual (G15.9+0.2) — stars: neutron — supernova remnants — X-rays: general — X-rays: ISM

1. INTRODUCTION

Supernovae and supernova remnants (SNRs) power Galactic turbulence and cosmic rays, drive Galactic chemical evolution, and illustrate the recent history of star formation. However, the Galaxy suffers a well-known shortage of young remnants. We are sure of only a few, whereas typical supernova rates (e.g., van den Bergh & Tammann 1991) predict three or more SNe per century, or 60 expected SNRs younger than 2000 yr. If we have not misunderstood Galactic supernova rates, star formation rates, or SNR evolution, then we are missing many young remnants.

Some of the missing young remnants may be concealed among known, but poorly studied, small-diameter radio remnants. We have begun a program to identify young SNRs by conducting observations with the *Chandra X-Ray Observatory* of several remnants with high radio surface brightnesses in order to obtain spectra to estimate ages and to search for evidence of ejecta. The first results of that program are presented in this Letter. The compact radio-bright remnant G15.9+0.2 reveals enhanced elemental abundances and has an inferred age of a few thousand years or less, making it one of the dozen or so youngest SNRs in the Galaxy. It is among the highest surface brightness radio SNRs in the Galaxy (see references in Green 2006) and has a fairly symmetrical radio shell structure (Fig. 1), both of which properties are indications of relative youth. We have also made the unexpected discovery of a central compact source in G15.9+0.2 that is likely to be associated with this remnant. If this is the case, we can identify G15.9+0.2 as the remnant of a core-collapse supernova.

The distance to G15.9+0.2 is poorly known, but there are several indications of a large distance, including a high absorption column density (verified by our spectral fits) and an estimate of 14 kpc from the (untrustworthy) Σ - D relation (see, e.g., Caswell et al. 1982, corrected to a galactocentric distance

of 8.5 kpc). In the absence of any other information, we scale all results for a fiducial distance of that to the Galactic center, 8.5 kpc. For this nominal assumed distance, the mean remnant radius is 6.2 pc.

2. OBSERVATIONS AND IMAGING

We observed G15.9+0.2 with *Chandra* using the ACIS-S CCD camera (S3 chip) on 2005 May 23 (10 ks), May 25 (5 ks), and May 28 (15 ks). We checked the aspect correction, removed pixel randomization in energy, corrected for charge transfer inefficiency, and filtered the light curve to reject background flares. We used calibration data from CALDB version 3.1.0. For spectral analysis, data were binned to a minimum of 25 counts per bin to allow the use of χ^2 statistics. Our source extraction region contained 32,000 counts (19,700 after background subtraction). Background was taken from essentially the entire area of the S3 chip not occupied by the source and not too near the chip edge. The relatively high percentage of background reflects Galactic ridge emission, along with the relatively low surface brightness of G15.9+0.2.

Figure 1 shows the *Chandra* image of G15.9+0.2, with radio contours. The shell is almost complete, with a very sharp outer edge. An unresolved source (hereafter CXOU J181852.0–150213) can be clearly seen in the interior, although well offset from the remnant center. The radio image was produced after reprocessing archival data obtained in 1993 at 1385 and 1465 MHz with the Very Large Array (VLA) in two hybrid configurations, BnC and CnD (Dubner et al. 1996). In addition to the 1.4 GHz image shown in Figure 1, we have also processed VLA data acquired in the direction of G15.9+0.2 at 327.5 and 5 GHz. No evidence of a radio counterpart for the central point source or for a radio flat-spectrum pulsar wind nebula (PWN) is evident in any of these radio images.

3. SPECTRAL ANALYSIS OF SNR SHELL

The integrated remnant spectrum is shown in Figure 2. Clearly apparent are the strong $K\alpha$ emission features of Mg, Si, S, Ar, and Ca and the effects of high interstellar absorption. The inte-

¹ Department of Physics, North Carolina State University, Raleigh NC 27695-8202; stephen_reynolds@ncsu.edu.

² NASA Goddard Space Flight Center, Code 660, Greenbelt, MD 20771

³ Instituto de Astronomía y Física del Espacio (IAFE), Casilla de Correos 67, Sucursal 28, 1428 Buenos Aires, Argentina.

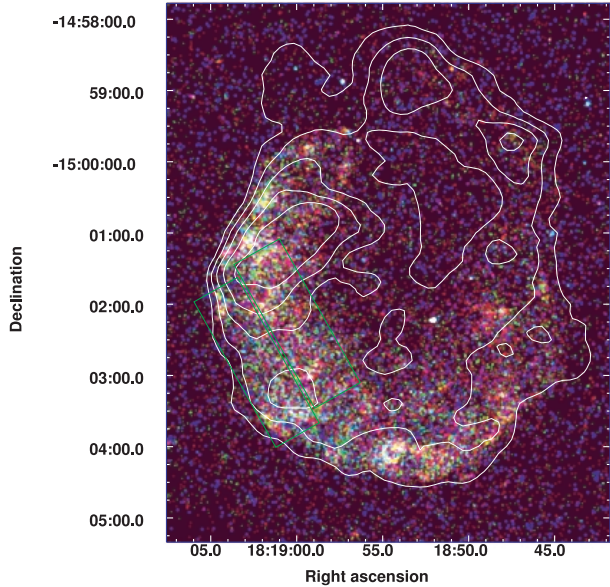


FIG. 1.—*Chandra* image of G15.9+0.2, with superposed radio contours. *Red*: 1–2 keV. *Green*: 2–3 keV. *Blue*: 3–7 keV. The image has been convolved with a $2''$ FWHM Gaussian. *Contours*: 1.4 GHz VLA image, resolution $12'' \times 5''$. Inner- and outer-shell regions described in the text are shown. The compact central source is the bright object slightly southwest of the shell center, at about $(18^{\text{h}}18^{\text{m}}52^{\text{s}}, -15^{\circ}02'14'')$.

grated remnant spectrum cannot be adequately fitted with a model for a planar shock with solar abundances (XSPEC model `ps shock`; Borkowski et al. 2001), but a model with variable abundances is much more successful (see Fig. 2; χ^2 moved from 378 to 245 for 233 degrees of freedom). The fitted column density of $N_{\text{H}} = (3.9 \pm 0.2) \times 10^{22} \text{ cm}^{-2}$ is relatively insensitive to the model (errors throughout are 90% confidence intervals). The electron temperature and ionization timescale are $kT_e = (0.9 \pm 0.1) \text{ keV}$ and $n_e t = 5.4 (4, 8) \times 10^{10} \text{ cm}^{-3} \text{ s}$, respectively. This model has a peculiar abundance pattern, requiring S and Ar at 2–5 times solar, but solar Si. Such an anomaly might arise if the spectrum were more complex than assumed, for instance, if there were actually two thermal components. We can obtain good fits ($\chi^2_{\nu} = 1.1$) with two components, one with solar abundances and the other with all abundances covaried (in solar ratios). Solar abundances in both components are ruled out at a high level of significance ($\Delta\chi^2 = 97$ with 235 degrees of freedom), but the amount of enhancement is strongly correlated with the emission measure (EM; the product of these quantities being roughly constant). The fitted absorption is consistent with the value given above for a single component. The solar and elevated-abundance components have temperatures of 0.7 (0.6, 0.9) and 2.3 (1.9, 3) keV, respectively, and ionization timescales of $7 (4, 12) \times 10^9$ and $6 (4, 8) \times 10^{10} \text{ cm}^{-3} \text{ s}$. The poorly constrained EM of the hotter component is an order of magnitude below that of the cool component for the 90% confidence lower limit on the enhancement (a factor of 10). The EM ($\equiv \int n_e n_{\text{H}} dV$) of the dominant cool component, $1.0 \times 10^{59} (D/8.5 \text{ kpc})^2 \text{ cm}^{-3}$, implies an rms electron density similar to that of the one-component model, about $3.8 (D/8.5 \text{ kpc})^{-1/2} \text{ cm}^{-3}$.

Supporting evidence for spatial variations in spectra comes from a separate examination of two regions southeast of the shell: one including the outer edge of emission, of width about $40''$ in the radial direction, and a second one inside the first, also of width $40''$ (Fig. 1). Fits to these two regions using `vp shock`

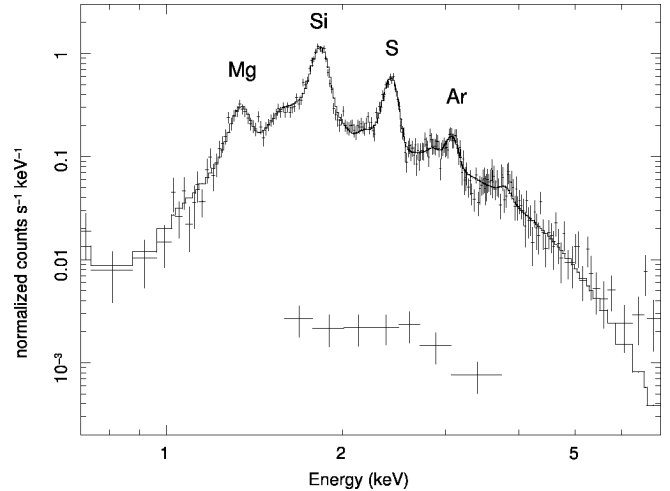


FIG. 2.—Integrated spectrum of G15.9+0.2, binned to a minimum of 25 counts per channel. *K α* lines of several elements are labeled. *Model*: Plane shock with variable abundances (`vp shock`). *Lower points*: Spectrum of central source, binned to 15 counts per channel.

(elements Mg, Si, S, Ar, and Ca allowed to vary in abundance) show significant differences (Fig. 3). In particular, the fitted ionization timescale for the outer region is $n_e t = 2 (0.5, 8) \times 10^{11} \text{ cm}^{-3} \text{ s}$, 6 times larger than that of the interior region. While the errors on fitted parameters are substantial, a fit to one spectrum when applied to the other increased χ^2 by 81 after renormalization (92 degrees of freedom; reduced χ^2 increased from 0.5 to 1.3). Furthermore, there is a suggestion of higher overabundances in the inner region: S about 3 times solar, Ar about

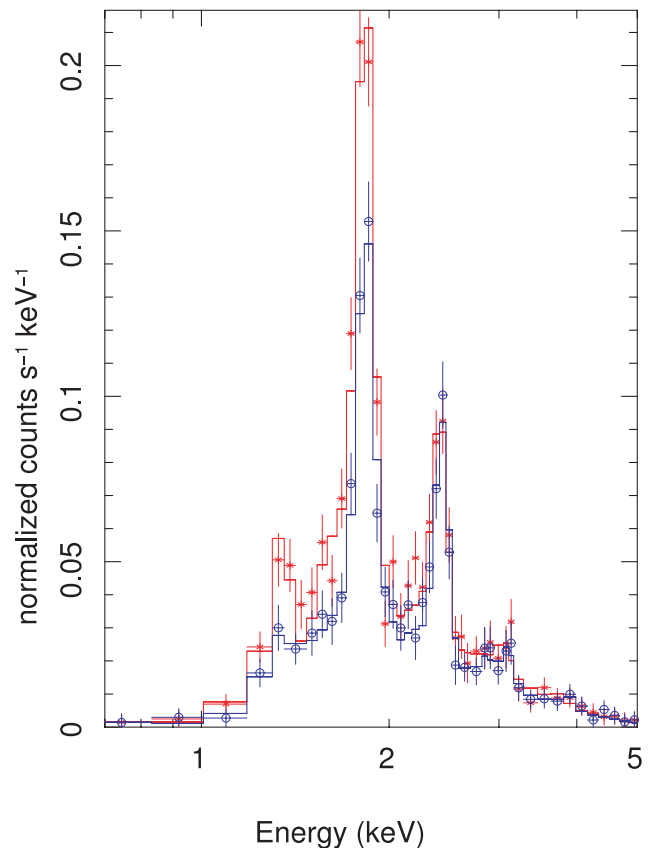


FIG. 3.—Spectra of outer (*blue circles*) and inner (*red points*) regions in southeast remnant. Note the clear spectral differences.

6 times, but with substantial errors. While these results do not constitute firm evidence of a distinct ejecta component, they do suggest it, and they indicate a spectral complexity in the remnant that is consistent with the relatively young age we infer below. A more complete understanding of the thermal shell emission in G15.9+0.2 will require a deeper observation, but this is not necessary for our general conclusions.

4. CXOU J181852.0–150213

The CXOU J181852.0–150213 emission is consistent with a point source and contains about 120 total counts in our observation (after background subtraction). The spectrum is highly absorbed with an N_{H} value consistent with that of the shell. We therefore froze N_{H} at the shell value of $3.9 \times 10^{22} \text{ cm}^{-2}$ for fitting of the CXOU J181852.0–150213 spectrum. We used Gehrels weighting of the data, appropriate for our count rates (Gehrels 1986), and binned the data to at least 15 counts per bin, resulting in only 7 bins (we have no evidence of counts below 1 keV). (Churazov weighting [Churazov et al. 1996], an alternative method for low count rate data, gave similar results.) A power-law fit gives a photon index $\Gamma \sim 3.8$ (3.1, 4.3). A blackbody fit with $kT = 0.4 \pm 0.1 \text{ keV}$ is equally acceptable. The inferred source flux is relatively insensitive to spectral parameters: $S_x \sim 1 \times 10^{-13} \text{ ergs cm}^{-2} \text{ s}^{-1}$ (2–9.5 keV) giving an X-ray luminosity in that energy range of $L_x \sim 10^{33} (D/8.5 \text{ kpc})^2 \text{ ergs s}^{-1}$. The total luminosity of a spherical blackbody with $kT \sim 0.4 \text{ keV}$ is $L_{\text{bb}} = 3.3 \times 10^{33} (R/10 \text{ km})^2 \text{ ergs s}^{-1}$. This luminosity is comparable to that of other point sources associated with SNRs, as we discuss below. The time resolution of CCD full-frame imaging observations is only 3.2 s, so it is impossible to search for the fast periods characteristic of normal pulsars. Furthermore, our sparse data are inadequate for period searches on longer timescales.

The source position (fit with *wavdetect*) is R.A. = $18^{\text{h}}18^{\text{m}}52.081 \pm 0.006$, decl. = $-15^{\circ}02'13.91 \pm 0.06$ (J2000). The quoted (1σ) errors reflect the statistical accuracy of the X-ray measurement only. The statistical error in the X-ray coordinate system registration is also 100 mas; we measured the position of a bright star visible in X-rays and shifted X-ray coordinates by a total of $79 \pm 102 \text{ mas}$ based on its second US Naval Observatory CCD Astroglyph Catalog (UCAC2) position (Zacharias et al. 2004). The combined 1σ statistical error is 150 mas. No other bright X-ray sources coincident with stars with accurate position are present in the *Chandra* field of view, so we cannot improve the coordinate registration accuracy or check for a potential rotation of *Chandra* images (but rotation errors are generally negligible).

We searched various catalogs for optical or IR counterparts within $2''$ of our best-fit position. There is a star $1''.0$ away to the south in the Galactic Legacy Infrared Mid-Plane Survey Extraordinaire (GLIMPSE) survey, which used *Spitzer's* Infrared Array Camera (IRAC; Benjamin et al. 2003), G015.8774+00.1966, and another fainter star $1''.9$ to the north, G015.8781+00.1970. These two stars have been detected in the IRAC channels 1 and 2 only (with effective wavelengths of 3.6 and 4.5 μm), and not at longer wavelengths. Their $m_{[3.6]}$, $m_{[4.5]}$ magnitudes are 13.0, 13.0 (G015.8774+00.1966) and 13.7, 13.8 (G015.8781+00.1970). At *Spitzer's* spatial resolution, these two stars blend together, with the X-ray source located between them. These two stars have no counterparts in the Two Micron All Sky Survey (2MASS) catalog of point sources, but their blend is faintly visible on images in all (*J*, *H*, and *K_s*) 2MASS bands. Nothing is visible at the X-ray source location on either optical sky survey images or in the *Spitzer* MIPS GAL survey of the inner Galactic plane at 24 and 70 μm .

The absence of a bright IR/optical counterpart rules out a stellar coronal origin for the detected X-ray source. The registration of the GLIMPSE and UCAC2 coordinate systems is accurate, as demonstrated by the small (200 mas) difference between GLIMPSE and UCAC2 coordinates of the reference star used to align the X-ray image. This difference is consistent with the internal GLIMPSE 1σ error of 100 mas for this star. The measurement error for G015.8774+00.1966 is comparable, so the total 1σ statistical error in the coordinate difference measurement between this star and the compact source does not exceed 200 mas. Because systematic errors are not expected to exceed statistical errors, the spatial offset between the two GLIMPSE stars and the X-ray source makes them unlikely candidates for the IR counterparts. Their presence in all 2MASS band images suggests that they are located much closer than G15.9+0.2. The high ($4 \times 10^{22} \text{ cm}^{-2}$) column density N_{H} toward G15.9+0.2 implies a very high ($A_V = 22 \text{ mag}$) optical extinction, and expected absorption is high even in the IR (6.2, 3.9, 2.5, 1.4, and 1.1 mag in *J*, *H*, *K_s*, [3.6], and [4.5] photometric IRAC bands, respectively; we used an IR extinction curve of Indebetouw et al. 2005). Such high extinction would cause reddening by 5.1 mag between the *J* and [3.6] bands, making detection of the faint 18 mag IR counterpart in the *J* band unlikely (the 2MASS Point Source Catalog sensitivity limit in this band is 15.8 mag at 99% completeness in regions of low stellar density). However, the two GLIMPSE stars are seen in all 2MASS bands, implying less extreme extinction (and hence a smaller distance than for G15.9+0.2). This and a lack of spatial alignment with the X-ray source strongly suggest that they are just two foreground stars projected against the SNR. An identification of an IR counterpart to the central compact X-ray source in G15.9+0.2 is not possible with either 2MASS or GLIMPSE data because of high spatial confusion in the Galactic plane and because of the relatively low sensitivity of these surveys. Deep near-IR observations with much better spatial resolution are necessary to identify the IR counterpart to the central compact X-ray source in G15.9+0.2.

Explanations other than the neutron star interpretation for CXOU J181852.0–150213 are unlikely, but they cannot be excluded without additional observations. At the observed 2–10 keV X-ray flux of $5 \times 10^{-14} \text{ ergs cm}^{-2} \text{ s}^{-1}$, most X-ray sources seen within the Milky Way are extragalactic, but with a nonnegligible contribution from low-luminosity Galactic X-ray sources such as cataclysmic variables (Hands et al. 2004). We expect only 0.01 sources with equal or larger fluxes in the central region of G15.9+0.2 encompassing CXOU J181852.0–150213, based on the count rate of 40 such sources per deg^{-2} measured by Hands et al. (2004). The power-law fit to the spectrum of CXOU J181852.0–150213 excludes at the 90% confidence level the typical value of $\Gamma \sim 2$ we would expect for an active galactic nucleus (AGN), although a deeper observation would be desirable to confirm this conclusion. An accurate measurement of the interstellar absorption would be very helpful in establishing the true nature of CXOU J181852.0–150213. Unfortunately, the current 90% confidence ranges for N_{H} are too broad [$(1.8\text{--}6.8) \times 10^{22} \text{ cm}^{-2}$ and $(3.8\text{--}13) \times 10^{22} \text{ cm}^{-2}$ for fits with the blackbody and the power law, respectively] to allow us to distinguish between various alternatives.

5. DISCUSSION AND CONCLUSIONS

We may attempt to estimate the age of G15.9+0.2 in various ways. Most directly, we assume an average time evolution of the shock radius of $R_s \propto t^m$, and take $R_s = 6.2(D/8.5 \text{ kpc}) \text{ pc}$, and

a shock velocity on the order of $u_8 \equiv v_s/(1000 \text{ km s}^{-1})$ based on measured gas temperatures above 0.7 keV. (In the absence of electron-ion temperature equilibration, the shock velocity would be higher, and the inferred age lower.) Assuming $m = 0.4$ as for Sedov evolution, we then find $t = 2400/u_8(D/8.5 \text{ kpc}) \text{ yr}$. If the remnant has not fully reached the Sedov stage, then $m > 0.4$, and this age is an upper limit. We can also use the Sedov relation $R_s = 1.15(E/\rho_0)^{1/5}t^{2/5}$ and an assumed explosion energy $E = 10^{51}$ ergs to estimate $t = 1400(D/8.5 \text{ kpc})^{9/4} \text{ yr}$. From the emission measure for the single-component fit, we estimate an upstream density of $n_0 \sim 0.7(D/8.5 \text{ kpc})^{-1/2} \text{ cm}^{-3}$ assuming a factor of 4 compression at the shock. The inferred swept-up mass is then $4\pi R_s^3 \rho_0/3 = 22(D/8.5 \text{ kpc})^{5/2} M_\odot$, which is comparable to the expected ejected mass for a core-collapse explosion, as required for the assumption of Sedov dynamics to be self-consistent. However, it is not much larger than that expected ejecta mass, consistent with a young age.

The upstream density and swept-up mass inferred from the solar-abundance component of our two-component fits are very similar to those found for the single-component fit, since the elevated-abundance component contributes little to the total emission measure. The age may also be estimated from the ionization age and the density as $t_s = n_e t/n_{\text{rms}} = 540(D/8.5 \text{ kpc})^{1/2} \text{ yr}$. Since the fitted values of the ionization age are less reliable than, say, the EM, it is not surprising that this estimate is somewhat different.

We consider the nature of the point source located inside G15.9+0.2. The compact source in G15.9+0.2 has properties that are typical of compact point sources associated with supernova remnants: a blackbody temperature of 0.4 keV and a luminosity of order $10^{33} \text{ ergs s}^{-1}$ (Pavlov et al. 2004). An association with the remnant is strengthened because the high absorption of the point source's spectrum implies that it and the remnant are at a comparable distance. The blackbody temperature, however, is too high for a normal cooling neutron star of any age (Yakovlev & Pethick 2004), and the low luminosity would require that the emission arise from only about 0.3% of the surface. This is a common property of the central compact object (CCO) class; in particular, thermal emission from small "hot spots" on the surface of a neutron star was proposed by Pavlov et al. (2000) to explain the low X-ray luminosity of the CCO in Cas A. Compared to anomalous X-ray pulsars (AXPs), our point source's luminosity is 1–2 orders of magnitude too low (Woods & Thompson 2006), and our data do not allow us to verify either the typical blackbody plus power-law spectrum or the long periodicities typical of AXPs. If we have underestimated the distance by a factor of 3–10, the luminosity would fall in the AXP class, but that would require G15.9+0.2 to be

at least 25 kpc away—an unlikely possibility. Magnetospheric emission from a rotation-powered pulsar may also explain the compact central source in G15.9+0.2. The observed L_x is typical of such objects, as is a power-law spectrum (although the slope in this case is somewhat steep). However, if the compact source is an active pulsar, it might be expected to produce a PWN. We see no evidence of extended emission around the source, although, as with other issues, a considerably deeper observation would be desirable. We consider a CCO or rotation-powered pulsar to be viable possibilities for the point source in G15.9+0.2.

If the compact source is indeed associated with G15.9+0.2, a somewhat high space velocity is required, assuming that it was born near the geometric center of the shell emission. Its current position is offset by about $35''$ from a visual estimate of the shell center, which translates to a sky-plane velocity of about $700(D/8.5 \text{ kpc})(t/2000 \text{ yr}) \text{ km s}^{-1}$, where t is the remnant age. While high, this velocity is not implausible, since as many as 15% of pulsars may be born with the implied three-dimensional spatial velocity required of over 1000 km s^{-1} (Arzoumanian et al. 2002); the CCO in Pup A has a directly measured velocity of order 1000 km s^{-1} (Winkler & Petre 2006; Hui & Becker 2006).

We conclude that G15.9+0.2 is probably no more than a few thousand years old, making it one of the 10 or 20 youngest remnants in the Galaxy. The tidy shell morphology is consistent with a young age, and our spectral analysis indicates enhanced abundances that are likely to be ejecta emission (although ambient abundances at the galactocentric radius of 2.4 kpc for G15.9+0.2 may be somewhat higher than locally). Ejecta emission alone does not demand extreme youth since several SNRs in the Galaxy and the LMC show detectable ejecta even at ages of order 10^4 yr (e.g., Hughes et al. 1995; Hendrick et al. 2003). Taken as a whole, with the low emitting mass and relatively low-ionization timescale, we are confident that G15.9+0.2 is a young remnant.

The compact object in G15.9+0.2 may be a candidate for addition to the very short list of CCOs in supernova remnants (Pavlov et al. 2004 cite six CCOs). Its age of 1000–3000 yr is comparable to that of several of the CCOs, as is its X-ray luminosity. The richness of the X-ray spectrum of the shell remnant indicates that a deeper X-ray observation could allow improved inferences on the remnant age and abundances. It would also clarify the nature of the central source, whether a PWN-less rotation-powered pulsar, a CCO, or a background AGN.

We thank the anonymous referee for a particularly thorough and helpful review. This work was supported by NASA through *Chandra* GO program grant GO5-6051A.

REFERENCES

- Arzoumanian, Z., Chernoff, D. F., & Cordes, J. M. 2002, *ApJ*, 568, 289
 Benjamin, R. A., et al. 2003, *PASP*, 115, 953
 Borkowski, K. J., Lyerly, W. J., & Reynolds, S. P. 2001, *ApJ*, 548, 820
 Caswell, J. L., Haynes, R. F., Milne, D. K., & Wellington, K. J. 1982, *MNRAS*, 200, 1143
 Churazov, E., Gilfanov, M., Forman, W., & Jones, C. 1996, *ApJ*, 471, 673
 Dubner, G. M., Giacani, E. B., Goss, W. M., Moffett, D. A., & Holdaway, M. 1996, *AJ*, 111, 1304
 Gehrels, N. 1986, *ApJ*, 303, 336
 Green D. A., 2006, *A Catalogue of Galactic Supernova Remnants* (2006 April Ver.; Cambridge: Astrophys. Group, Cavendish Lab.) <http://www.mrao.cam.ac.uk/surveys/snrs/>
 Hands, A. D. P., Warwick, R. S., Watson, M. G., & Helfand, D. J. 2004, *MNRAS*, 351, 31
 Hendrick, S., Borkowski, K., & Reynolds, S. 2003, *ApJ*, 593, 370
 Hughes, J. P., et al. 1995, *ApJ*, 444, L81
 Hui, C. Y., & Becker, W. 2006, *A&A*, 454, 543
 Indebetouw, R., et al. 2005, *ApJ*, 619, 931
 Pavlov, G. G., Sanwal, D., & Teter, M. A. 2004, in *IAU Symp.* 218, *Young Neutron Stars and Their Environments*, ed. F. Camilo & B. M. Gaensler (San Francisco: ASP), 239
 Pavlov, G. G., Zavlin, V. E., Aschenbach, B., Trümper, J., & Sanwal, D. 2000, *ApJ*, 531, L53
 van den Bergh, S., & Tammann, G. 1991, *ARA&A*, 29, 363
 Winkler, P. F., & Petre, R. 2006, *ApJL*, submitted (astro-ph/0608205)
 Woods, P. M., & Thompson, C. 2006, in *Compact Stellar X-Ray Sources*, ed. W. H. G. Lewin & M. van der Klis (Cambridge: Cambridge Univ. Press), 547
 Yakovlev, D. G., & Pethick, C. J. 2004, *ARA&A*, 42, 169
 Zacharias, N., Urban, S. E., Zacharias, M. I., Wycoff, G. L., Hall, D. M., Monet, D. G., & Rafferty, T. J. 2004, *AJ*, 127, 3043